An Adaptive Control Scheme for Local and Coordinated Ramp Metering

Maria Kontorinaki*, Iasson Karafyllis†, Markos Papageorgiou* and Yibing Wang‡

*Dynamic Systems & Simulation Laboratory, Technical University of Crete, Chania, Greece 73100
Email: mkontorinaki@dssl.tuc.gr, markos@dssl.tuc.gr
† Dept. of Mathematics, National Technical University of Athens, Athens, Greece, 15780, Email: iasonkar@central.ntua.gr
‡Inst. of Transportation Engineering, Zhejiang University, Hangzhou, China, 310058, Email: wangyibing@zju.edu.cn

Abstract—This study aims to provide insights and demonstrate the properties and the performance of a nonlinear adaptive control scheme which has been recently developed to address the ramp metering problem arising in freeways. The proposed scheme consists of a nominal feedback law in conjunction with a nonlinear observer which aims to estimate some unknown system variables. A distinguishing novelty of the proposed approach is that it can inherently be applied both at local and coordinated levels. The control scheme is tested for realistic traffic scenarios using a macroscopic traffic flow simulator as a surrogate for potential field application. Comparison tests have been performed with other control strategies proposed in the literature and employed already in the field.

I. INTRODUCTION

Ramp metering is an effective control measure for freeway networks, which aims at ameliorating traffic conditions by appropriately regulating the inflow from the on-ramps. However, the goal of such control measures can only be achieved if driven by an opportune control strategy [1]. Real-time (traffic-responsive) ramp metering strategies, fed with real-time measurements from sensors installed in the freeway network and the on-ramps, are considered to be the most robust and efficient approach in this context.

Real-time ramp metering strategies can be classified as local (demand-capacity strategy and its variations [2], ALINEA strategy and its variations [3],[4], neural network [5] and fuzzy logic based [6] approaches) or coordinated (optimal control strategies [7], [8], [9], linear multivariable control strategies [10], rule-based algorithms [11]). There exist also mixed ramp metering strategies such as [12]. The ultimate goal of any of the above ramp metering control strategies is to real-time determine, in the most efficient way, the inflows from the on-ramps, when congestion phenomena are present or imminent at the corresponding mainstream region, so as to maximize freeway throughput.

Recently, an Adaptive Control Scheme (ACS) has been proposed in [13] as a real-time ramp metering strategy, which can be applied either at local or coordinated levels. The proposed ACS has been developed on the basis of general freeway models, developed in [14], which are generalizations of the well-known first-order discrete Godunov approximation of the LWR model ([15], [16]). In particular, the ACS consists of two main components: i) a Nominal Feedback Law (NFL) in conjunction with ii) a nonlinear observer that estimates the unknown system parameters utilized by the NFL. In [14], it has been rigorously shown that the nominal feedback law guarantees the robust, global exponential stabilization of any selected uncongested model equilibrium point when the model parameters are known and constant. In [13], a nonlinear dead-beat observer was designed, which performs the exact identification of the constant model parameters after a transient period. The combined implementation of these two components constitutes the proposed ACS which guarantees the robust global exponential attractivity of the desired (partly unknown) uncongested (moving) equilibrium point [13].

Motivated by the aforementioned strong theoretical properties of the ACS, this work aims to provide insights in its practical properties and performance under realistic and customary freeway traffic scenarios. Testing this strategy with sufficiently accurate traffic flow models, different than the ones used for ACS design, is deemed as an indispensable step towards potential application of the scheme in the field. In this study, the simulation model METANET [17], which is able to reproduce with high accuracy the traffic dynamics [18], is utilized as a surrogate of ground truth for the application of the ACS. First, the performance of the control scheme is investigated with respect to the stabilization of freeway traffic in case bottlenecks exist far downstream from a metered on-ramp. Second, by appropriately exploiting the application flexibility provided by ACS, the scheme is applied for coordinated ramp metering control, so as to balance the relative queue lengths created on the controllable on-ramps.

The rest of the paper is organized as follows. Section II is devoted to the detailed description of the ACS. Section III briefly describes the simulation setting, while the application results of the ACS at local and coordinated ramp metering levels are presented in Sections IV and V, respectively. The main conclusions are given in Section VI.

II. THE ADAPTIVE CONTROL SCHEME (ACS)

The proposed ACS aims to delay, prevent or dissolve congestion phenomena caused by the presence of recurrent active bottlenecks (on-ramp merging areas, lane drops, tunnels, bridges) within a freeway stretch. By its nature, any real-time control strategy requires measurements of flow, speed or density, obtained from appropriately located detectors within the freeway. On the other hand, if the required measurements

are deficient or absent, then appropriate estimation schemes can be used so as to retrieve the necessary traffic flow information from available measurements [19].

As mentioned above, the ACS consists of two main components, a NFL and a nonlinear observer. The first aims to steer the system towards a desired traffic state while the second aims to estimate the external traffic variables required for producing the desired traffic state. The following subsection presents the NFL component under the assumption that all the required measurements or estimates are available.

A. The Nominal Feedback Law (NFL)

To enable the real-time operation of the NFL, real-time information of traffic density should be available. If there are no density measurements, density estimates can be readily obtained from corresponding (usually available) occupancy measurements or can be provided by various estimation schemes [20], [19]. In what follows, the measurements or estimates of density are in [veh/km]. Although other configurations are possible, we will consider a freeway traffic control setting that is compatible with the cases addressed in [4] for isolated ramp metering and in [12] for coordinated ramp metering. Thus, we are in a position to have a reference point for comparison.

1) Main features of the Nominal Feedback Law: A freeway stretch under control extends from the most upstream controllable on-ramp until a recurrently activated bottleneck at its downstream boundary (Fig. 1), in the aim of maximizing bottleneck throughput. The freeway stretch may contain other controllable or uncontrollable on-ramps, as well as off-ramps. A space discretization of the considered freeway stretch is introduced with cells which are typically about 500 m in length. Let n be the total number of cells emerging after discretizing the freeway; the nth (last) cell corresponds to the bottleneck cell. The on-ramps and the off-ramps are located at the upstream and downstream boundary of a cell, respectively, and are denoted by the index $i \in \{1,...,n\}$ of the corresponding cell. Let $O \subseteq \{1,...,n\}$ be the index set of the on-ramps and let $R \subseteq O$ be the index set of the controllable on-ramps. Then, u_i denotes the controllable inflow of on-ramp $i \in R$ and r_i denotes the actual inflow of on-ramp $i \in O$; in case $i \in R$, the actual inflow r_i depends on the control decision and therefore becomes $r_i(u_i)$ (Fig. 1). All flows are measured in [veh/h]. The upstream-most boundary cell is denoted by the index $i = 0$. Let T_c be the control holding period and let T be the measurement (or estimate) sampling period, where $T_c = z_c T$ with $z_c \in \mathbb{N}$. With these definitions, the control action (at times $t = k_c T_c$, with $k_c = 1, 2, ...$) ordered by the NFL reads:

$$u_i(k_c) = \max\left(u_i^{min}, u_i^*(k_c) - \frac{u_i^*(k_c) - u_i^{min}}{\tau} \Xi\big(\rho(k_c)\big)\right), \quad (1)$$

for $i \in R$, where

$$\Xi\big(\rho(k_c)\big) = \sum_{j=1}^{n} \sigma^j \max\big(0, \rho_j(k_c) - \rho_j^*(k_c)\big), \quad (2)$$

where $u_i^{min} > 0$ is the minimum admissible on-ramp flow, $\sigma \in (0,1]$ (dimensionless) and $\tau > 0$ (in [veh/km]) are parameters of the regulator, $\rho_j(k_c)$ $(j = 1,...,n)$ correspond to (the average of the last z_c) density measurements or estimates and $(u_i^*(k_c), \rho_j^*(k_c))$ $(i \in R, j = 1,...,n)$ denotes the Desired Operating Point (DOP), reflecting optimal non-congested conditions in the examined freeway stretch.

The efficient operation of the NFL (1), (2) requires the proper determination of the regulator parameters σ and τ. In fact, the NFL assigns a different control gain to each cell j of the considered freeway stretch, which is equal to σ^j/τ (σ^j denotes σ to the power of j). However, simulation experiments indicate that the selection $\sigma = 1$ (yielding the same control gain, i.e., $1/\tau$ for each freeway cell) and appropriate determination of the parameter τ guarantees satisfactory control performance. Typical values for τ may be selected within the range [1,30]; whereby smaller values of τ lead to more aggressive (even oscillating) control behavior, while larger values of τ lead to less aggressive (but possibly sluggish) control behavior. In any case, tuning of only one design parameter is sufficient to establish the desired dynamic characteristics of the control loop, and this is certainly a convenient feature for practical application of the method.

The determination of the DOP (u_i^*, ρ_j^*) $(i \in R, j = 1,...,n)$ is crucial and is based on two aspects: i) the maximization of throughput at the bottleneck location (cell n) and ii) the uncongested equilibrium flow along the considered freeway.

2) Maximization of throughput at the bottleneck location: In order to determine the DOP, the knowledge of the bottleneck's critical density ρ_n^{cr} (density at which flow reaches capacity) will be assumed. The proper critical density value should be extracted from historical data or be specified after the control installation via fine-tuning. Then, in order to achieve maximization of throughput, we define the target outflow q_n^* of the freeway stretch (which turns out to be the estimate of the capacity flow of the bottleneck location) as

$$q_n^*(k_c) = \rho_n^{cr} v_n(k_c), \quad (3)$$

where $v_n(k_c)$ (in [km/h]) is the measured or real-time estimated mean speed at the bottleneck. The target outflow given by (3) may lead to unrealistically high estimated capacity values whenever the measured or estimated speed is near free speed. However, in such cases no control actions will be considered since the freeway operates under free flow conditions. On the other hand, when the real density approaches its critical value, the mean speed reduces approaching the "critical speed" and the estimate (3) is close to the real capacity value.
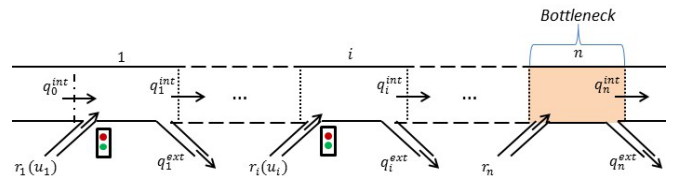

Fig. 1. Space discretization of a freeway stretch.

3) Equilibrium flow: The DOP (u_i^*, ρ_j^*) ($i \in R$, $j = 1, ..., n$) implies the balance between the total inflows and the total outflows (along with the target outflow (3)) in the considered freeway stretch. Specifically, the total inflows comprise: i) the optimal inflows u_i^* of the controllable on-ramps ($i \in R$); ii) the measured or estimated uncontrollable on-ramp flows r_i ($i \in O \backslash R$); and iii) the very upstream, measured or estimated, mainstream inflow q_0^{int}, i.e., the outflow from cell $i = 0$ that becomes inflow for cell $i = 1$. The total outflows comprise: i) the measured or estimated external (off-ramp) flows q_j^{ext} ($j = 1, ...n$), expressed as the product of the corresponding estimated exit rates p_j, $j \in \{1, ..., n\}$, with the corresponding mainstream flows (in case cell j does not contain an off-ramp, we set $p_j = 0$); and ii) the target outflow of the bottleneck q_n^*. Then, the equilibrium flow for the uncongested freeway stretch (updated at every control time step k_c) yields:

$$q_n^* = q_0^{int} \prod_{j=1}^{n} (1-p_j) + \sum_{i \in R} u_i^* \prod_{j=i}^{n} (1-p_j) + \sum_{i \in O \backslash R} r_i \prod_{j=i}^{n} (1-p_j) \tag{4}$$

with $p_n = 0$. Notice that the only unknown variables within (4) are the optimal inflows for the controllable on-ramps ($u_i^*; i \in R$). Thus, (4) allows to specify these optimal inflows, at each control time step k_c, with $m - 1$ degrees of freedom, where m is the number of controllable on-ramps i.e., the cardinality of the index set R. In case there is just one controllable inflow (local ramp metering case), relation (4) can be solved to retrieve the optimal inflow value $u_1^*(k_c)$. For more than one controllable on-ramps, the user has the freedom to specify the way that the optimal inflow values should be distributed among the controllable on-ramps (see, e.g., Section V). Thus, this control scheme allows dealing with a variety of possible coordinated ramp-metering policies when more than one on-ramps are controllable. Note that the specified values of ($u_i^*; i \in R$) should not be selected higher than the on-ramps capacity or lower than u_i^{min}.

4) Final determination of the desired operating point: Finally, the corresponding equilibrium densities $\rho_j^*(k_c)$ are given by:

$$\rho_n^*(k_c) = \rho_n^{cr}, \quad \rho_j^*(k_c) = \min\left(\frac{q_j^*(k_c)}{v_j(k_c)}, \rho_j^{cr}\right), j=1, ..., n\text{-}1, \tag{5}$$

where $v_j(k_c)$ and ρ_j^{cr} correspond again to the measured or real-time estimated mean speed and the critical density of the jth cell, respectively, and $q_j^*(k_c)$ are given by:

$$q_1^* = q_0^{int} + u_1^*, \tag{6}$$

$$q_j^* = q_0^{int} \prod_{k=1}^{j-1} (1\text{-}p_k) + \sum_{\substack{i \in R \\ i \le j}} u_i^* \prod_{k=i}^{j-1} (1\text{-}p_k) + \sum_{\substack{i \in O \backslash R \\ i \le j}} r_i \prod_{k=i}^{j-1} (1\text{-}p_k) \tag{7}$$

for $j = 2, ..., n - 1$, where we set $\prod_{k=j}^{j-1} \cdot = 1$.

To summarize, in order to apply the NFL, we need measurements or estimates of: a) all cell densities ($\rho_i; i = 1, ..., n$) and b) external variables for deriving the DOP, namely, i)

uncontrollable on-ramp flows ($r_i; i \in O \backslash R$), ii) cell speeds ($v_j; j = 1, ..., n$), iii) the exit rates ($p_j; j = 1, ..., n-1$) and iv) uncontrollable mainstream inflow (q_0^{int}). All these quantities may be delivered by appropriate estimation schemes (e.g., [20], [19]), however, in [13], a specific estimation scheme that is dedicated to the present traffic control problem and specifically concerns the real-time estimation of the external variables i), ii) and iii) above, has been proposed and is presented in the next subsection.

B. The Nonlinear Observer

In [13], a parameter vector to be estimated is defined which includes, as mentioned above, the external variables i), ii) and iii); while the mainline inflow q_0^{int} is assumed to be known (measured). This estimation scheme utilizes density measurements or estimates, ρ_j, as well as internal cell flow measurements or estimates, q_j^{int} (flow that exits from cell j and becomes inflow for the next cell $j+1$), and external (off-ramp) flow measurements, q_j^{ext} (for every $j = 1, ..., n$). In what follows, the estimated quantities are denoted by ($\hat{r}_i; i \in O \backslash R$), ($\hat{v}_j; j = 1, ..., n$) and ($\hat{p}_j; j = 1, ..., n$), respectively. Then, the nonlinear observer reads:

$$\hat{r}_i(k_c) = \begin{cases} U_i(k_c) & \rho_{i-1}(k_c) < \rho_{i-1}^{cr} \text{ and } \rho_i(k_c) < \rho_i^{cr} \\ \hat{r}_i(k_c\text{-}1) & \text{otherwise} \end{cases}, \tag{8}$$

$$\hat{v}_i(k_c) = \begin{cases} V_i(k_c) & 0 < \rho_i(k_c) < \rho_i^{cr} \text{ and } \rho_{i+1}(k_c) < \rho_{i+1}^{cr} \\ \hat{v}_i(k_c\text{-}1) & \text{otherwise} \end{cases}, \tag{9}$$

$$\hat{p}_i(k_c) = \begin{cases} P_i(k_c) & q_i^{int}(k_c) + q_i^{ext}(k_c) > 0 \\ \hat{p}_i(k_c\text{-}1) & \text{otherwise} \end{cases}, \tag{10}$$

where

$$U_i(k_c) = \frac{L_i}{T_c}(\rho_i(k_c)\text{-}\rho_i(k_c\text{-}1)) + q_i^{int}(k_c\text{-}1) + q_i^{ext}(k_c\text{-}1) - q_{i-1}^{int}(k_c\text{-}1)), \tag{11}$$

$$V_i(k_c) = \frac{q_i^{int}(k_c) + q_i^{ext}(k_c)}{\rho_i(k_c)}, \tag{12}$$

$$P_i(k_c) = \frac{q_i^{ext}(k_c)}{q_i^{int}(k_c) + q_i^{ext}(k_c)}. \tag{13}$$

Relations (8), (9), (11) and (12) indicate that the estimated values of each uncontrollable inflow and mean speed are updated only if the densities of the corresponding cells and the upstream or downstream cells, respectively, are undercritical. The estimation of the uncontrollable inflows is performed by means of a conservation equation, and the resulting values are truncated if they exceed a maximum admissible value r_i^{max} (on-ramp's capacity) or zero. The estimates of mean speed correspond to the ration of flow over density which are also truncated between v_i^{min} and v_i^{max} which are pre-specified constants denoting the minimum and maximum expected speed, respectively. Relations (10) and (13) indicate that the estimated values for the exit rates are updated only for positive total exit flows.

III. SIMULATION SETTING

The well-known macroscopic traffic flow simulator METANET [17] is utilized for the simulation tests of the following sections. METANET employs a second-order traffic flow model consisting of two interconnected dynamic equations which describe the evolution of traffic density and mean speed, respectively. Modeling details can be found in [17].

For simulation purposes the time and space arguments are discretized. Specifically, the simulated freeway stretch is divided into N cells, where for each cell i, the model describes the dynamic behavior of traffic flow during the time period $[kT, (k+1)T]$, with $k = 0, 1, 2....$. Notice here that the last freeway cell n, considered as the bottleneck cell in the previous section, is not necessarily identical with the last cell of the simulation model, i.e., $n \leq N$.

For the on-ramps as well as for the mainstream entrance flow, a simple queue model is used in METANET. The evolution of the on-ramp queue w_i is described by an additional state (conservation) equation which reads:

$$w_i(k+1) = w_i(k) + T\big(d_i(k) - r_i(k)\big), \qquad (14)$$

where d_i denotes the external traffic demand of the on-ramp $i \in O$. The above equation will be used in Section V for deriving a queue balancing control strategy.

For the local ramp metering results of Section IV, the control scenario as well as the network topology, the model parameters and the (deterministic or stochastic) demand scenarios are precisely the same with those adopted in [4]. For the coordinated ramp metering results of Section V, the control scenario is the same with the one adopted in [12]. For both cases, the simulation time step, the control time step and the simulation horizon are equal to $T = 5$ s, $T_c = 30$ s and $T_{hor} = 5$ h, respectively. Moreover, the regulator parameters are identical in all experiments conducted and equal to $\sigma = 1$ and $\tau = 10$ [veh/km/lane], indicating the low sensitivity of the ACS with respect to its control gains.

The control algorithm is the same for both scenarios. Summarizing, measurements of flow and density (specifically, $\rho_i(k)$, $q_0^{int}(k)$, $q_i^{int}(k)$, $q_i^{ext}(k)$, for each cell i of the considered freeway stretch), stemming from METANET simulator, are extracted every $T = 5$ s. Then, the average of these measurements are fed to the observer (8)-(13) and the NFL (1), (2) every $T_c = 30$ s. The observer estimates the unknown external variables (exit rates, mean speeds and uncontrollable on-ramp inflows) which are then fed to (3) and (4) in order to obtain the optimal inflows for the controllable on-ramps, u_i^*, for $i \in R$. In case there are more than one controllable on-ramps, an additional decision policy (see Section V) is required to exploit the additional degrees of freedom. The obtained optimal inflow values are subsequently utilized by (5)-(6) for the calculation of the equilibrium densities ρ_j^*, for each j of the freeway stretch. Finally, the produced DOP (u_i^*, ρ_j^*) is fed to the NFL (1), (2) which in turn feeds back the simulation model with the control decisions. This control loop is activated every $T_c = 30$ s.

Lastly, we note that no maximum on-ramp queues have been considered in the investigated scenarios so as to focus on the impact of the ACS application to the mainstream conditions.

IV. LOCAL RAMP METERING

In many practical cases, bottlenecks with smaller capacity than the merging area may exist further downstream for various reasons. In [4] the performance of the control strategy ALINEA and its extension PI-ALINEA were investigated with respect to the existence of such bottlenecks created by lane-drops, curvatures or uncontrolled on-ramps. In this section, the performance of the proposed ACS in such cases is investigated.

A. Network description

For the simulation tests, two freeway stretches with $N = 22$ cells have been considered (Fig. 2). Each stretch has an on-ramp located at the upstream boundary of cell 9, which is 2 km downstream from the network entrance. Each cell is $L_i = 0.25$ km and has $l_i = 3$ lanes. The first network (Fig. 2(a)) does not involve any downstream bottleneck; however, the on-ramp's merge area itself is a bottleneck. In order to distinguish this network from the other, it is referred hereafter as the non-bottleneck case. The other network has a 1 km bottleneck at 1.5 km downstream of the on-ramp (Fig. 2(b)). A bottleneck cell differs from a non-bottleneck cell in traffic flow characteristics. In particular, a flow-density relation (Fundamental Diagram - FD), with lower capacity compared to non-bottleneck cells, has been considered for bottleneck cells. For each of these networks, no control and control results are presented. Moreover, realistic conditions, whereby the traffic demand is corrupted with noise and the model equations include noise terms, are also presented.

B. Non bottleneck case

The non-bottleneck case is first considered for the application of the ACS. Due to the complex nonlinear dynamics of the macroscopic simulation model, the factual critical density of a simulated freeway stretch is not the same with the critical density considered in the FD of the simulation model. For this case, the factual critical density is found to be around 38 [veh/km/lane]. The density and flow trajectories, for the no control case, are shown in Figs. 3(a) and (b), respectively. The total demand entering the merging cell (mainstream and on-ramp), during the peak period, exceeds considerably the capacity of cell 9, which is around 6000 [veh/h]. Fig. 3(a) shows that as the density continues to increase beyond 38 [veh/km/lane], congestion builds in cell 9 spilling back
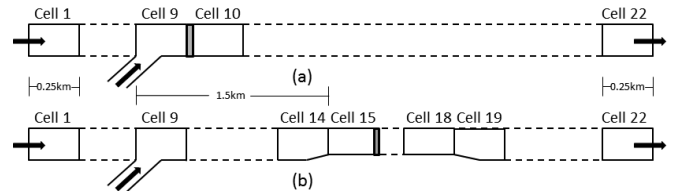

Fig. 2. Freeway stretches: (a) non-bottleneck case and (b) bottleneck case.
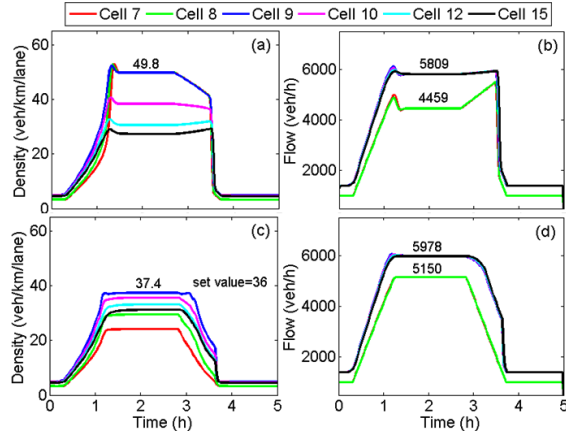
Fig. 3. Non-bottleneck case: (a) density and (b) flow in the no control case, (c) density and (d) flow with application of the ACS.

upstream. Thus, the outflow of cell 9 and the downstream cells drops to around 5800 [veh/h] (capacity drop).

Here, the considered freeway stretch for the application of the ACS contains only cell 9. Then, the observer of the ACS is employed only for the estimation of mean speed at cell 9. The optimal inflow, according to (3) and (4), is set equal to $u_9^*(k_c) = \rho_9^{cr}\hat{v}_9(k_c)l_9 - q_8^{int}(k_c)$. Figs. 3(c) and (d) display the density and flow trajectories, respectively, for $\rho_9^{cr} = 36$ [veh/km/lane]. Hereafter, the critical density of the bottleneck cell which is fed to the ACS value is called the set-point. A small offset between the set-point and the resulting stationary density is produced by the application of ACS. Therefore, the selected set-point is the most efficient resulting to the desired capacity flow. This offset is a natural consequence of the modeling mismatch (recall that the development of ACS has been based on first-order models). This implies that some fine-tuning may be also required for the set-point value in case of ACS field implementation for maximum efficiency.

Generally, ACS is seen to respond very satisfactorily, and no congestion is created in cell 9 or elsewhere. More specifically, Fig. 4(c) indicates that density trajectories are identical to those in the no-control case until the density of cell 9 reaches the factual critical density value, after which all density trajectories are stabilized during the whole peak period. In particular, the density of cell 9 is kept at 37.4 [veh/km/lane], leading to: i) a stable capacity flow downstream of the on-ramp that accommodates all the entrance demand; and ii) a controlled peak-period on-ramp flow, which establishes the desired freeway throughput (capacity flow). Clearly, the ramp metering actions lead to the formation and, eventually, dissipation of ramp queue, since the allowed on-ramp inflow is less than the on-ramp demand during the peak period. It is also noted that, due to the almost 2.9% higher outflow from the merging cell (compare Fig. 3(b) and Fig. 3(d)), the density under the action of ACS, becomes undercritical much earlier than in the no-control case, i.e., the demand is served earlier. Thus, the ramp metering action leads to the corresponding reduction of the total time spent by all vehicles, including the

queuing at the ramp. Furthermore, it is also interesting to see that no oscillations in the density trajectories at the cells close to the on-ramp are observed.

C. Bottleneck case

For the bottleneck case, shown in Fig. 2(b), the factual critical density and the corresponding capacity of the bottleneck cells are found to be around 41 [veh/km/lane] and 5270 [veh/h], respectively. The sum of the mainstream and the on-ramp demand during peak period is higher than the bottleneck capacity, but is definitely lower than the merging area capacity. The congestion is expected to appear first in cell 15, and the ramp metering target is to keep the bottleneck flow (rather than the merging cell flow) around its capacity level. Figs. 4(a) and (b) show the density and flow trajectories for the no-control case, where, indeed, the congestion occurs first in the corresponding bottleneck cell and spills back upstream. During the whole peak period, the flow downstream of the on-ramp is lower (5188 [veh/h], in Fig. 4(b)) than the bottleneck capacity, due to capacity drop caused by the congestion.

The considered freeway stretch for the application of ACS extends from cell 9 to cell 15. Due to the fact that there are no intermediate on-ramps and off-ramps, the observer of the ACS is called to estimate only the mean speeds of the cells of the considered freeway stretch. Then, the optimal inflow is $u_9^*(k_c) = \rho_{15}^{cr}\hat{v}_{15}(k_c)l_{15} - q_8^{int}(k_c)$.

The testing results of the ACS are presented in Figs. 4(c),(d). The set-point used is $\rho_{15}^{cr} = 41$ [veh/km/lane]. A very small offset is present also here. The congestion formation and propagation from the bottleneck cells to the upstream cells are prevented. A small overshooting is observed at the initial phase
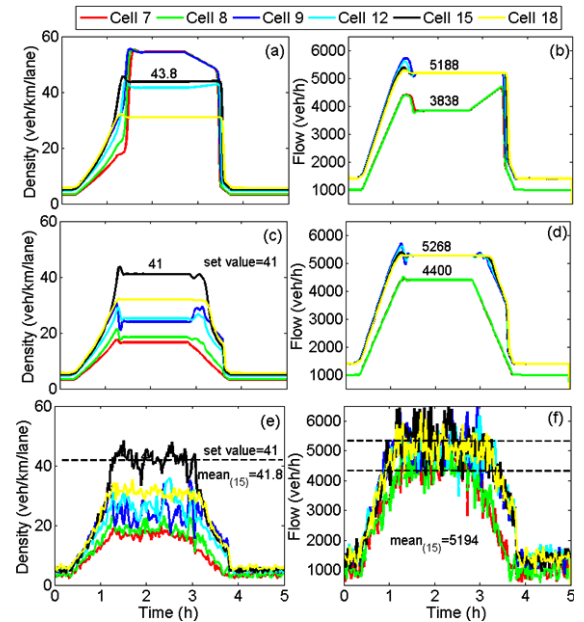

Fig. 4. Bottleneck case: (a) density and (b) flow in the no-control case, (c) density and (d) flow with application of the ACS, (e) density and (f) flow with the application of the ACS under stochastic demands and process noise.

of control activation, which, however is deemed minor and is actually virtually masked by the noise in the stochastic version of this scenario (Figs. 4 (e), (f)). In fact, the trajectory of the density in cell 15 is smooth after a short transient period with the small overshooting. In the steady state, the density of cell 15 is kept around the factual critical density, while the capacity level of the bottleneck cells is achieved, and the mainstream demand is well served. Furthermore, high-frequency demand and process noise are taken into account by testing ACS with a more realistic stochastic scenario. Also, in this scenario, the density of cell 9 is kept near critical (its mean during the peak period is equal to 41.8 [veh/km/lane], see Fig. 4 (e)). The merge cell throughput remains high at the peak period (see Fig. 4 (f)) and the entrance flow demand is fully served.

The investigations reported in this section demonstrate that ACS is efficient for local ramp metering where the bottleneck location may be either the on-ramp merge area or another tighter bottleneck farther downstream. Two different cases of bottleneck locations have been addressed with equal design parameters for ACS. Since the same cases had also been considered in [4] by use of PI-ALINEA, a visual comparison with the results presented therein indicate similar performance, in fact with slightly better damped transient control period in the case of ACS.

V. COORDINATED RAMP METERING

In this section, ACS is tested as a control strategy for coordinated ramp metering. A freeway stretch of $N = 13$ cells is considered. Each cell is $L_i = 0.5$ km and has $l_i = 3$ lanes (Fig. 5). Each freeway cell is described by the same FD. There are two on-ramps on this freeway as well as an off-ramp in-between. For the simulation tests, the exit rate at the off-ramp is set to $p_6 = 5\%$. The total flow demand arriving at the upstream boundary of cell 9, during the peak period, exceeds the capacity flow of cell 9, and therefore cell 9 is a bottleneck for the freeway. The factual critical density and the corresponding capacity flow of cell 9 are about 39 [veh/km/lane] and 6130 [veh/h], respectively.

When no control is applied, the resulting density and flow profiles for both merge areas and also other cells of the freeway are shown in Figs. 6 (a) and (b). As expected, mainstream congestion appears after 1 h in the merge area of on-ramp 9 due to the high flows that arrive there; this leads to a visible mainstream flow decrease (capacity drop). The created congestion travels upstream and reaches the merge area of on-ramp 5 at around 2 h, also leading to a visible flow decrease. No queues are formed at the on-ramps, but a small queue is created at the upstream entrance of the simulated network.
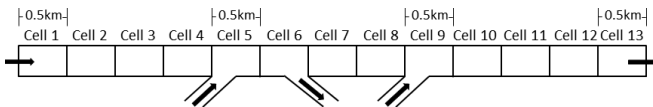

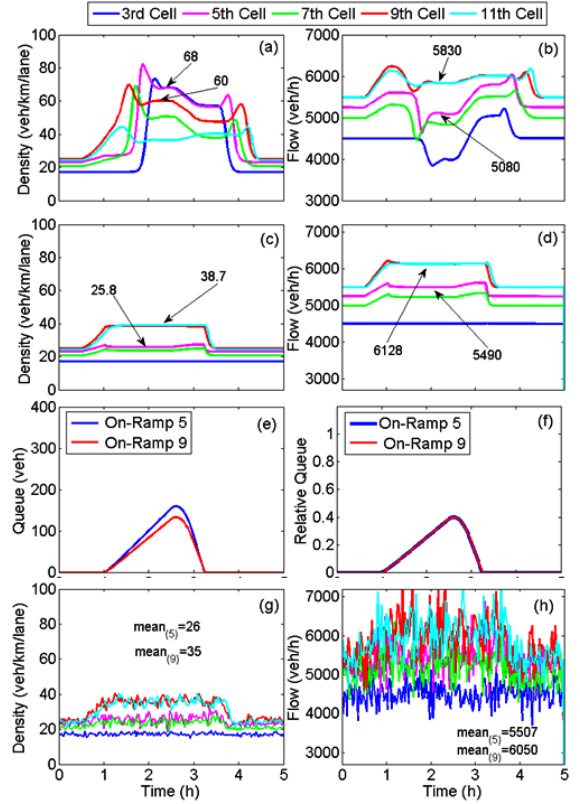Fig. 5. Freeway stretch for the coordinated ramp metering scenario.

Fig. 6. (a) Density and (b) flow in the no control case and (c) density and (d) flow with application of the ACS.

ACS is employed in order to simultaneously control both on-ramp flows so as to maximize throughput right after on-ramp 9. The considered freeway stretch for control extends from cell 5 to cell 9. Due to the fact that there are no intermediate on-ramps within this stretch, the observer of ACS is only employed in order to estimate mean speeds of the cells of the considered freeway stretch as well as the exit rate from off-ramp 6. The optimal inflow values, u_5^* and u_9^*, must be appropriately determined. The remaining degree of freedom shall be used to balance dynamically the relative lengths of the created queues (if any) on both controllable on-ramps. To this end, a second relationship, along with (3), that associates the optimal inflows is needed. This relationship may be directly derived from the target of balancing the relative ramp queues, i.e.,

$$\frac{w_5(k_c)}{w_5^{max}} = \frac{w_9(k_c)}{w_9^{max}}, \qquad (15)$$

where w_5^{max} and w_9^{max} are the maximum admissible on-ramp queues (in [veh]) for the two on-ramps. Substituting (14) into (15) and replacing r_5 and r_9 with u_5^* and u_9^* respectively, a relationship between the optimal inflows is obtained. Then, using also relation (3), the optimal inflow values can be uniquely determined. More specifically, let us introduce, for convenience, the following notations:

$$A(k_c) = \rho_9^{cr}\hat{v}_9(k_c)l_9 - (1 - \hat{p}_6(k_c))q_4^{int}(k_c), \qquad (16)$$

$$A_1(k_c){=}w_5(k_c){-}T_c d_5(k_c),\ A_2(k_c){=}w_9(k_c){-}T_c(d_9(k_c){-}A(k_c)). \tag{17}$$

Then, the optimal inflows are given by:

$$u_5^*(k_c) = \frac{1}{T_c}\frac{w_9^{max}A_1(k_c) - w_5^{max}A_2(k_c)}{(1-\hat{p}_6)(k_c)w_5^{max} + w_9^{max}}, \tag{18}$$

$$u_9^*(k_c) = A(k_c) - (1-\hat{p}_6(k_c))u_5^*(k_c). \tag{19}$$

For this test, the maximum ramp queue lengths considered for relative queue balancing are $w_5^{max} = 200$ [veh] and $w_9^{max} = 167$ [veh]. Figs. 6 (c) and (d) present the density and flow profiles with the application of ACS. For this test, the set-point value is equal to $\rho_9^{cr} = 38$ [veh/km/lane], resulting again to a small off-set which leads the density of cell 9 near to its factual critical density. It can be seen from Fig. 6(c) that congestion is avoided and the maximization of throughput is achieved. Regarding the balancing of on-ramp queues, Figs. 6 (e) and (f) show the evolution of both the queue lengths and the relative queue lengths for the two on-ramps. On-ramp 5 has larger capacity, and therefore the queue formation there is larger than at on-ramp 9. However, the relative queue lengths are equal during the whole simulation horizon as desired.

In order to test the performance of the proposed coordination scheme with respect to stochastic scenarios, appropriate simulations have been conducted which are presented in Figs. 6 (g) and (h). As shown by these figures, the performance of the ACS is not affected by the presence of noise. Again, no congestion is formed along the freeway stretch (the mean of the density of cell 9 is undercritical, see Fig 6(g)), while the outflow from cell 9 is kept near capacity (its mean is almost 6050 veh/h, see Fig. 6(h)).

The scenarios investigated in this section demonstrate that ACS is also efficient for coordinated ramp metering. As mentioned above, similar cases, with the ones utilized in this study, had also been considered in [12] by use of a linked-control strategy. By comparing (again visually) the results therein with the reported results in this study, we conclude that no important differences in the performance of the two control strategies exist. However, ACS is simpler in application than many existing coordination schemes, including the one presented in [12].

VI. Conclusions

The reported investigations evidence that ACS is applicable, at will, as a local and coordinated ramp metering strategy, and that acts efficiently in both cases task, leading to damped and satisfactory control results. The utilization of the same regulator parameters for various scenarios indicates that little fine-tuning will be necessary in potential field applications. A little fine-tuning may be required for the selection of the set-point density due to the offset produced with the application of ACS.

Acknowledgment

References

[1] M. Papageorgiou and A. Kotsialos, "Freeway ramp metering: An overview," *IEEE Transactions on Intelligent Transportation Systems*, vol. 3, pp. 271–281, 2002.

[2] D. P. Masher, D. W. Ross, P. J. Wong, P. L. Tuan, H. M. Zeidler, and S. Petracek, "Guidelines for design and operation of ramp control systems," *Transportation Research Board*, 1975.

[3] M. Papageorgiou, H. Hadj-Salem, and J.-M. Blosseville, "ALINEA: A local feedback control law for on-ramp metering," *Transportation Research Record*, no. 1320, pp. 58–64, 1991.

[4] Y. Wang, E. Kosmatopoulos, M. Papageorgiou, and I. Papamichail, "Local ramp metering in the presence of a distant downstream bottleneck: Theoretical analysis and simulation study," *IEEE Transactions on Intelligent Transportation Systems*, vol. 15, pp. 2024–2039, 2014.

[5] H. M. Zhang and S. Ritchie, "Freeway ramp metering using artificial neural networks," *Transportation Research Part C: Emerging Technologies*, vol. 5, pp. 273–286, 1997.

[6] S. Vukanovic and O. Ernhofer, "Field evaluation of the fuzzy logic based ramp metering algorithm accezz," in *Proceedings of the 11th IFAC Symposium on Control Transportation Systems*, August 29-31, Delft, The Netherlands, 2006, pp. 119–123.

[7] T. Bellemans, B. De Schutter, and B. De Moor, "Model predictive control with repeated model fitting for ramp metering," in *Proceedings of the IEEE 5th International Conference on Intelligent Transportation Systems*, September 3-6, Singapore, 2002, pp. 236–241.

[8] A. Hegyi, B. De Schutter, and J. Heelendoorn, "MPC-based optimal coordination of variable speed limits to suppress shock waves in freeway traffic," in *Proceedings of the American Control Conference*, June 4-6, Denver, Colorando, USA, 2003, pp. 4083–4088.

[9] G. Gomes and R. Horowitz, "Optimal freeway ramp metering using the asymmetric cell transmission model," *Transportation Research Part C: Emerging Technologies*, vol. 14, pp. 244–262, 2006.

[10] M. Papageorgiou, J. M. Blosseville, and H. Haj-Salem, "Modelling and real-time control of traffic flow on the southern part of boulevard priphrique in paris: Part II: Coordinated on-ramp metering," *Transportation Research Part A: General*, vol. 24, pp. 361–370, 1990.

[11] J. Hourdakis and P. Michalopoulos, "Evaluation of ramp control effectiveness in two twin cities freeways," *Transportation Research Record*, no. 1811, pp. 21–29, 2002.

[12] I. Papamichail and M. Papageorgiou, "Traffic-responsive linked ramp-metering control," *IEEE Transactions on Intelligent Transportation Systems*, vol. 9, pp. 111–121, 2008.

[13] I. Karafyllis, M. Kontorinaki, and M. Papageorgiou, "Robust global adaptive exponential stabilization of discrete-time systems with application to freeway traffic control," *to appear in the IEEE Transactions on Automatic Control, doi 10.1109/TAC.2017.2699125*, 2017.

[14] ——, "Global exponential stabilization of freeway models," *International Journal of Robust and Nonlinear Control*, vol. 26, pp. 1184–1210, 2016.

[15] M. J. Lighthill and G. B. Whitham, "On kinematic waves II: A theory of traffic flow on long crowded roads," *Proceedings of the Royal Society of London A*, vol. 229, pp. 317–345, 1955.

[16] P. I. Richards, "Shock waves on the highway," *Operations research*, vol. 4, pp. 42–51, 1956.

[17] A. Messmer and M. Papageorgiou, "METANET: A macroscopic simulation program for motorway networks," *Traffic Engineering and Control*, vol. 31, pp. 466–470, 1990.

[18] M. Kontorinaki, A. Spiliopoulou, C. Roncoli, and M. Papageorgiou, "Capacity drop in first-order traffic flow models: Overview and real-data validation," in *Proceedings of the 95th Annual Transportation Research Board Meeting*, no. 16-3541, Washington, D.C., USA, 2016.

[19] Y. Wang, M. Papageorgiou, and A. Messmer, "RENAISSANCE: A unified macroscopic model-based approach to real-time freeway network traffic surveillance," *Transportation Research Part C: Emerging Technologies*, vol. 14, pp. 190–212, 2006.

[20] N. Bekiaris-Liberis, C. Roncoli, and M. Papageorgiou, "Highway traffic state estimation with mixed connected and conventional vehicles using speed measurements," in *Proceedings of the IEEE 18th International Conference on Intelligent Transportation Systems*, September 15-18, La Palmas de Gran Canaria, Spain, 2015, pp. 2806–2811.